HDR TOMOGRAPHY VIA MODULO RADON TRANSFORM

Matthias Beckmann[†,⋆], Felix Krahmer[‡] and Ayush Bhandari[⋆]

[†] Dept. of Mathematics, University of Hamburg, Bundesstraße 55, 20146 Hamburg, Germany.
[‡]Dept. of Mathematics, Technical University of Munich, Garching 85747, Germany.
[⋆] Dept. of Electrical and Electronic Engineering, Imperial College London, SW72AZ, UK.

Emails: matthias.beckmann@uni-hamburg.de • felix.krahmer@tum.de • a.bhandari@imperial.ac.uk

ABSTRACT

The topic of high dynamic range (HDR) tomography is starting to gain attention due to recent advances in the hardware technology. Registering high-intensity projections that exceed the dynamic range of the detector cause sensor saturation. Existing methods rely on the fusion of multiple exposures. In contrast, we propose a one-shot solution based on the Modulo Radon Transform (MRT). By exploiting the modulo non-linearity, the MRT encodes folded Radon Transform projections so that the resulting measurements do not saturate. Our recovery strategy is pivoted around a property we call compactly λ-supported, which is motivated by practice; in many applications the object to be recovered is of finite extent and the measured quantity has approximately compact support. Our theoretical results are illustrated by numerical simulations with an open-access X-ray tomographic dataset and lead to substantial improvement in the HDR recovery problem. For instance, we report recovery of objects with projections 1000x larger in amplitude than the detector threshold.

Index Terms— Computational imaging, computer tomography, high dynamic range, Radon transform and sampling theory.

1. INTRODUCTION

Computerized tomography (CT) has revolutionized medical imaging. At the heart of the CT technology is the Radon Transform, although the roots of this topic date back to the work of Minkowski who first proposed the idea of recovering mathematical objects, given its line integrals over big circles on a sphere. Funk tackled this problem for the case of the sphere [1] and Radon solved the problem with respect to Euclidian spaces [2]. Fast forward 100 years and a series of engineering marvels, the CT technology has become the most powerful tool to image human beings in a non-invasive fashion.

Despite the remarkable progress on the front of algorithm design, the pace of hardware evolution for this technology has been relatively slow-moving. Until now, in most settings, the CT hardware was assumed to be fixed and the ideology was to concentrate efforts on the algorithmic aspects. That said, there are certain lossy aspects of data acquisition that cannot be handled easily using algorithms. One such problem is that of the dynamic range. Almost all physical sensors have a fixed operating range. Physical entities such as voltage, amplitude or intensity that exceed this threshold cause the sensor to saturate resulting in a permanent information loss.

As the imaging technology is constantly being pushed to its peak, only recently the practitioners have started to think about *high dynamic range* (HDR) tomography — recovery of images where the dynamic range far exceeds the sensor's recordable threshold. To this end, Chen et al. [4] proposed the idea of HDR image reconstruction. Their key idea relies on the conventional HDR imaging setup which exploits multiple, low dynamic range images at different exposure levels which are then combined algorithmically to yield a HDR image. In the context of CT, Chen et al. obtained multiple exposures by varying the tube-voltage. Eppenberger et al. [6] extended this idea to the case of colored imaging. Weiss et al. [7] proposed a pixel-level design for HDR X-ray imaging. Extending the idea of Chen et al. [4], in [5] Li et al. proposed an approach to automate the exposure level of each image used for HDR X-ray reconstruction.

Taking a different approach to this problem, the authors of the current paper proposed the Modulo Radon Transform (MRT) in [8] as a conceptual alternative to the conventional Radon Transform. The MRT is similar to the Radon Transform in that, at each orientation, it computes line integrals in the Euclidean space. However, instead of recording the Radon Transform projections, the MRT records the remainders with respect to the maximum recording voltage, λ. Hence, the MRT encodes measurements using the modulo non-linearity. The distinct *advantage* of this computational imaging centric approach is that the encoded measurements, which are always in the range of $[-\lambda, \lambda]$, can be reliably acquired far beyond the dynamic range of a conventional ADC; hence, sensor saturation or clipping as they appear in the scenarios discussed in [4–7] is circumvented. That said, MRT encoded measurements lead to a new format of information loss; a smooth function is converted into its discontinuous counterpart. To undo the effect of the modulo non-linearity, the authors in [8] describe a decoding algorithm which is guaranteed to succeed provided that the smoothness is preserved via inter-sample correlation; this leads to an upper-bound on the sampling rate while requiring infinitely many samples.

Practical Implementation and Feasibility. Some readers may wonder how this non-linearity is to be put into practice. Semiconductor imaging sensors that implement folding for HDR imaging have been around since early 2000 (cf. [12]). Their link with modulo non-linearities and the related inverse problem of signal reconstruction was recently studied in a line of work on *Unlimited Sampling* [9–11]. Beyond imaging hardware, [7] clearly shows that HDR X-ray imaging is possible via pixel-level customization. A confluence of [7] and [9] may potentially result in a new tomography hardware capable of implementing the ideas underlying the *Modulo Radon Transform* [8].

Contributions. In this paper, we propose a novel reconstruction technique for HDR tomography based on the Modulo Radon Transform. The MRT as defined in [8] is a conceptual tool and works
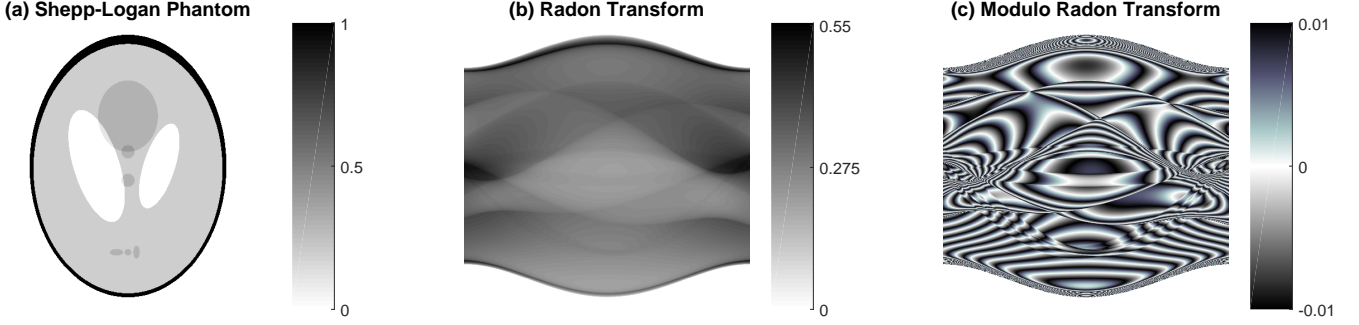
Fig. 1. The Modulo Radon Transform converts high dynamic range tomographic information into low dynamic range samples. (a) The Shepp-Logan phantom, (b) Conventional Radon Transform and (c) Modulo Radon Transform with $\lambda = 0.01$.

for functions on $\mathbb{R}^2$ (infinite sample sizes). In contrast, here, we develop a reconstruction strategy that can handle finite sample sizes, which is the case in practice. To make it practically amenable to applications, we resort to a tool we refer to as λ-support. This may be interpreted as an approximately compact support and allows us to show how Radon Projections can be exactly recovered from Modulo Radon Projections while using much less samples than our previously developed algorithm in [8]. The target function is then approximated by applying filtered back projection to the recovered Radon Projections, which leads to a reconstruction of the same quality as for conventional Radon data.

We illustrate our theoretical results with a real Radon dataset example, where our current approach to MRT is able to compress the dynamical range of the Radon projections by about 500 times and the increase in sample size is only one fifth compared to our earlier work in [8].

2. MODULO RADON TRANSFORM

Let $f \equiv f(\mathbf{x})$ be the two-dimensional function or image in our setup with spatial coordinates $\mathbf{x} = (x_1, x_2)^\top \in \mathbb{R}^2$. For given $\lambda > 0$, we consider the problem of recovering f from its Modulo Radon data

$$\left\{ \mathscr{R}^\lambda f\left(\boldsymbol{\theta}, t\right) \mid \left(\boldsymbol{\theta}, t\right) \in \mathbb{S}^1 \times \mathbb{R} \right\}$$

with the *Modulo Radon Transform* $\mathscr{R}^\lambda f : \mathbb{S}^1 \times \mathbb{R} \longrightarrow [-\lambda, \lambda]$ given by

$$\mathscr{R}^\lambda f\left(\boldsymbol{\theta}, t\right) = \mathscr{M}_\lambda \left(\mathcal{R} f\left(\boldsymbol{\theta}, t\right)\right).$$

Here, $\mathscr{M}_\lambda$ denotes the centered 2λ-modulo operation with

$$\mathscr{M}_\lambda (t) = 2\lambda \left(\left[\!\left[\frac{t}{2\lambda} + \frac{1}{2} \right]\!\right] - \frac{1}{2} \right),$$

where $[\![t]\!] = t - \lfloor t \rfloor$ is the fractional part of t. Moreover, $\mathcal{R} f$ is the conventional Radon Transform of $f \in L^1\left(\mathbb{R}^2\right)$ with

$$\mathcal{R} f\left(\boldsymbol{\theta}, t\right) = \int_{\ell_{t,\boldsymbol{\theta}}} f(\mathbf{x}) \, d\mathbf{x},$$

which computes the line integral along the line $\ell_{t,\boldsymbol{\theta}}$ that is perpendicular to $\boldsymbol{\theta} = (\cos(\theta), \sin(\theta))$ with $\theta \in [0, 2\pi)$ and has distance t from the origin. For fixed $\theta \in [0, 2\pi)$ we set

$$\mathcal{R}_\theta f = \mathcal{R} f\left(\boldsymbol{\theta}, \cdot\right) \quad \text{and} \quad \mathscr{R}_\theta^\lambda f = \mathscr{R}^\lambda f\left(\boldsymbol{\theta}, \cdot\right).$$

Since $\mathcal{R}$ satisfies the evenness condition $\mathcal{R} f\left(-\boldsymbol{\theta}, -t\right) = \mathcal{R} f\left(\boldsymbol{\theta}, t\right)$, it suffices to collect the data at projection angles $\theta \in [0, \pi)$.

For illustration, Fig. 1 shows the Shepp-Logan phantom f_{SL} together with its Radon Transform $\mathcal{R} f_{\text{SL}}$ and its Modulo Radon Transform $\mathscr{R}^\lambda f_{\text{SL}}$ with threshold $\lambda = 0.01$. In this example, the MRT is able to compress the dynamic range of $\mathcal{R} f_{\text{SL}}$ by about 25 times.

The Modulo Radon Transform measurements are converted to a discrete-time form via a generalized sampling operation yielding the Modulo Radon Projections

$$p_\theta^\lambda [k] = \mathscr{M}_\lambda \left(\int_{\mathbb{R}} \mathcal{R}_\theta f(t) \, \phi(k\mathrm{T} - t) \, dt \right) = p_\theta^\lambda (k\mathrm{T}).$$

Here T is the sampling rate of the kernel $\phi \in L^2(\mathbb{R})$ which characterizes the impulse response of the detector used for data acquisition at different projection angles $\theta \in [0, 2\pi)$.

In this paper, we assume that ϕ is given by the ideal low-pass filter $\Phi_\Omega \in \mathrm{PW}_\Omega$ of bandwidth $\Omega > 0$ and propose the following sampling architecture for obtaining Modulo Radon samples in the dynamical range $[-\lambda, \lambda]$ with given threshold $\lambda > 0$:

(i) For fixed angle $\theta \in [0, \pi)$ we start with the one-dimensional projection $\mathcal{R}_\theta f \in L^1(\mathbb{R})$ to be sampled.

(ii) Pre-filtering of $\mathcal{R}_\theta f$ with $\Phi_\Omega \in \mathrm{PW}_\Omega$ results in the Radon Projection $p_\theta \in \mathrm{PW}_\Omega$ given by

$$p_\theta (t) = \left(\mathcal{R}_\theta f * \Phi_\Omega\right)(t) = \int_{\mathbb{R}} \mathcal{R}_\theta f(s) \, \Phi_\Omega (t - s) \, ds.$$

(iii) The Radon Projection p_θ is folded in the range $[-\lambda, \lambda]$ via the centered 2λ-modulo mapping $\mathscr{M}_\lambda$ resulting in

$$p_\theta^\lambda (t) = \mathscr{M}_\lambda \left(p_\theta (t)\right).$$

(iv) Finally, the Modulo Radon Projection p_θ^λ is sampled with sampling rate $\mathrm{T} > 0$ yielding uniform samples

$$p_\theta^\lambda [k] = p_\theta^\lambda (k\mathrm{T}) = \mathscr{M}_\lambda \left(p_\theta (k\mathrm{T})\right).$$

If the function f is itself band-limited with bandwidth Ω, the pre-filtering step (ii) does not change the data and we have

$$p_\theta (t) = \mathcal{R}_\theta f(t).$$

In applications, however, we deal with compactly supported functions f that cannot be band-limited. In this case, the Radon projection $p_\theta \in \mathrm{PW}_\Omega$ has essentially compact support in the sense that for any $c > 0$ there is $t_c > 0$ such that $|p_\theta (t)| < c, \ \forall \, |t| > t_c$. In the following, we assume that f is supported in $B_1(0)$, i.e.,

$$f(\mathbf{x}) = 0 \quad \forall \, \|\mathbf{x}\|_2 > 1.$$

Moreover, in practice only finitely many samples of p_θ^λ are taken for finitely many angles $\theta \in [0, \pi)$. Here, we assume that we are given Modulo Radon Projections

$$\left\{ p_{\theta_m}^\lambda(t_k) \mid -K \leq k \leq K, \ 0 \leq m \leq M-1 \right\}$$

in parallel beam geometry with $t_k = k\,\mathrm{T}$ and $\theta_m = m\,\frac{\pi}{M}$, where $\mathrm{T} > 0$ is the spacing of $2K+1$ parallel lines per angle.

To deal with this, we propose a sequential reconstruction approach, which we name *US-FBP method*. In the first step, we apply Unlimited Sampling (US) for what we call compactly λ-supported functions to recover p_θ from p_θ^λ for each angle θ. This will be explained in detail in Section 3. In the second step, we recover f from p_θ by applying the approximate filtered back projection (FBP) formula

$$f_\Omega = \frac{1}{2}\,\mathcal{R}^\#\left(F_\Omega * p_\theta\right), \tag{1}$$

where $F_\Omega \in \mathsf{PW}_\Omega$ is a reconstruction filter of the form

$$\mathcal{F}_1 F_\Omega(\omega) = |\omega|\,W(\omega/\Omega)$$

with even window $W \in L^\infty(\mathbb{R})$ supported in $[-1, 1]$ and $\mathcal{R}^\# h$ is the *back projection* of $h \equiv h(\boldsymbol{\theta}, t)$ defined as

$$\mathcal{R}^\# h(\mathbf{x}) = \frac{1}{2\pi}\int_{\mathbb{S}^1} h\left(\boldsymbol{\theta}, \mathbf{x}^\top \boldsymbol{\theta}\right)\,d\boldsymbol{\theta}.$$

As Φ_Ω and F_Ω have the same bandwidth, formula (1) can be rewritten as

$$f_\Omega = \frac{1}{2}\,\mathcal{R}^\#\left(F_\Omega * \mathcal{R}_\theta f\right)$$

and provides a band-limited approximation $f_\Omega \in \mathsf{PW}_\Omega$ to f with

$$\mathcal{F}_2 f_\Omega(\boldsymbol{\omega}) = W\left(\|\boldsymbol{\omega}\|_2/\Omega\right)\mathcal{F}_2 f(\boldsymbol{\omega}).$$

It is discretized using a standard approach and according to [15, Section 5.1.1], the optimal sampling conditions for fixed bandwidth $\Omega > 0$ are given by $\mathrm{T} \leq \pi/\Omega$, $K \geq 1/\mathrm{T}$, $M \geq \Omega$.

3. UNLIMITED SAMPLING OF COMPACTLY λ–SUPPORTED FUNCTIONS

The goal of this section is to outline a guaranteed algorithm that can recover finitely many samples $\gamma[k] = g(k\mathrm{T})$ with sampling rate $\mathrm{T} > 0$, given its modulo samples $y[k] = \mathscr{M}_\lambda(g[k])$. Our approach involves the forward difference operator $\Delta : \mathbb{R}^{d+1} \longrightarrow \mathbb{R}^d$, $(\Delta a)[k] = a[k+1] - a[k]$ and the corresponding anti-difference operator $\mathsf{S} : \mathbb{R}^d \longrightarrow \mathbb{R}^{d+1}$, $(\mathsf{S}a)[k] = \sum_{j=1}^{k-1} a[j]$, so that $\mathsf{S}(\Delta a) = a - a[1]$. Further, we use the modulo decomposition [10]

$$g(t) = \mathscr{M}_\lambda(g(t)) + \varepsilon_g(t), \tag{2}$$

where ε_g is a piecewise constant function with values in $2\lambda\mathbb{Z}$. We set $\varepsilon_\gamma[k] = \varepsilon_g(k\mathrm{T}) = \gamma[k] - y[k]$. We will make two assumptions on our function: $g \in \mathsf{PW}_\Omega$ is Ω-band-limited and *approximately* compactly supported. That latter condition makes sense since in the context of tomography the functions of interest live on a finite domain. The precise meaning of approximate compact support is clarified below in Definition 1 where we define the λ-support Property.

Definition 1 (λ-support Property). *Let $\lambda > 0$ and $g : \mathbb{R} \longrightarrow \mathbb{R}$ be a univariate function. We call g compactly λ-supported if there is $\rho > 0$ such that $|g(t)| < \lambda$ for $|t| > \rho$. In this case we write $g \in \mathcal{B}_\lambda^\rho$.*

Algorithm 1 Unlimited sampling of λ-supported functions

Input: samples $y[k] = \mathscr{M}_\lambda(g(k\mathrm{T}))$ for $k = -K', \ldots, K$, upper bound $\beta_g \geq \|g\|_\infty$

1: **choose** $N = \left\lceil \dfrac{\log(\lambda) - \log(\beta_g)}{\log(\mathrm{T}\Omega e)} \right\rceil_+$

2: $s_{(0)}[k] = \left(\Delta^N \varepsilon_\gamma\right)[k] = \left(\mathscr{M}_\lambda\left(\Delta^N y\right) - \Delta^N y\right)[k]$

3: **for** $n = 0, \ldots, N-2$ **do**

4: $\quad s_{(n+1)}[k] = 2\lambda\left\lceil \dfrac{\left\lfloor \mathsf{S}s_{(n)}[k]/\lambda \right\rfloor}{2} \right\rceil$ $\qquad \triangleright$ (rounding to $2\lambda\mathbb{Z}$)

5: **end for**

6: $\gamma[k] = y[k] + \left(\mathsf{S}s_{(N-1)}\right)[k]$

Output: samples $\gamma[k] = g(k\mathrm{T})$ for $k = -K, \ldots, K$

We remind the reader that when dealing with a finite number of samples, a recovery algorithm for compactly supported functions was proposed in [13, 14] in the context of sparse and parametric functions. However, by relaxing the compact support constraint by the λ-support property, we can work with significantly smaller sample sizes. This is the key benefit of this paper which is also very relevant to the practical setup of tomography.

Our recovery strategy is summarized in Algorithm 1 and exploits the observation that higher order finite-differences of smooth functions can be made to shrink arbitrarily. This result is summarized in the form of the following Lemma proved in [9, 10].

Lemma 1. *For $g \in \mathsf{PW}_\Omega$, the samples $\gamma[k] = g(k\mathrm{T})$ satisfy*

$$\|\Delta^N \gamma\|_\infty \leq (\mathrm{T}\Omega e)^N \|g\|_\infty.$$

Thus, once the sampling rate is chosen so that $(\mathrm{T}\Omega e)^N < \lambda/\beta_g$, we can extract $\Delta^N \gamma$ from folded samples y because at this sampling rate it is guaranteed that

$$\Delta^N \gamma = \mathscr{M}_\lambda\left(\Delta^N \gamma\right) = \mathscr{M}_\lambda\left(\Delta^N y\right).$$

Based on this observation, we now show that when $g \in \mathsf{PW}_\Omega \cap \mathcal{B}_\lambda^\rho$, Algorithm 1 recovers the samples $\gamma[k]$ exactly if we have enough modulo samples $y[k]$. How much is enough? This is answered by the next theorem.

Theorem 1. *Let $g \in \mathsf{PW}_\Omega \cap \mathcal{B}_\lambda^\rho$ and let $\mathbb{R}_{>0} \ni \beta_g \geq \|g\|_\infty$ be given. Then, a sufficient condition for the* exact *recovery of the samples $\gamma[k] = g(k\mathrm{T})$, $k = -K, \ldots, K$, from modulo samples $y[k] = \mathscr{M}_\lambda(g(k\mathrm{T}))$, $k = -K', \ldots, K$, using Algorithm 1 is given by*

$$\mathrm{T} \leq \frac{1}{2\Omega e} \quad and \quad K' \geq \max\left\{K, \rho\mathrm{T}^{-1} + N\right\},$$

where

$$N = \left\lceil \frac{\log(\lambda) - \log(\beta_g)}{\log(\mathrm{T}\Omega e)} \right\rceil_+.$$

Sketch of Proof for Theorem 1. If $\beta_g \leq \lambda$, the statement is trivially true. Thus, we assume $\beta_g > \lambda$. By the choice of T and N we have $(\mathrm{T}\Omega e)^N \leq \lambda/\beta_g$ and Lemma 1 ensures that $\|\Delta^N \gamma\|_\infty \leq \lambda$. This implies $\Delta^N \gamma = \mathscr{M}_\lambda\left(\Delta^N \gamma\right) = \mathscr{M}_\lambda\left(\Delta^N y\right)$ and, hence,

$$\left(\Delta^N \varepsilon_\gamma\right)[k] = \left(\mathscr{M}_\lambda\left(\Delta^N y\right)\right)[k] - \left(\Delta^N y\right)[k]$$
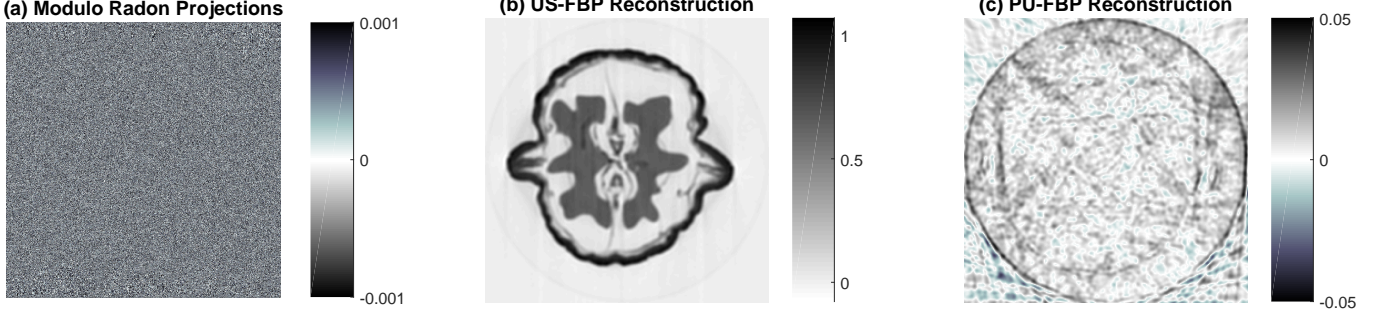
can be computed from $y[k]$, $k \in [-K', K]$.

Fig. 2. HDR tomography for walnut Radon data. (a) MRT with $\lambda = 0.001$ leads to 500-times compression in dynamic range. (b) US-FBP recovers the walnut by compensating the information loss with oversampling of factor $2\pi e$. (c) PU-FBP is not able to recover the walnut.

Since $g \in \mathcal{B}_\lambda^\rho$ and $K' \geq \rho T^{-1} + N$, we have

$$\varepsilon_\gamma\left[-K'\right] = g\left(-K'T\right) - \mathscr{M}_\lambda\left(g\left(-K'T\right)\right) = 0$$

and, for all $1 \leq n \leq N$,

$$\left(\Delta^n \varepsilon_\gamma\right)\left[-K'\right] = \sum_{m=0}^{n} \binom{n}{m} (-1)^{n-m} \varepsilon_\gamma\left[-K' + m\right] = 0.$$

With this, we show by induction in m that $s_{(m)} = \Delta^{N-m}\varepsilon_\gamma$. The induction seed reduces to the definition of $s_{(0)} = \Delta^N \varepsilon_\gamma$. For the induction step, we assume that for fixed m we have $s_{(m)} = \Delta^{N-m}\varepsilon_\gamma = \Delta(\Delta^{N-(m+1)}\varepsilon_\gamma)$. Then, applying the anti-difference operator S yields, $\mathsf{S}s_{(m)} = \Delta^{N-(m+1)}\varepsilon_\gamma$. In particular, we have $\left(\mathsf{S}s_{(m)}\right)[k] \in 2\lambda\mathbb{Z}$ and indeed obtain

$$s_{(m+1)} = 2\lambda \left\lceil \frac{\lfloor \mathsf{S}s_{(m)}/\lambda \rfloor}{2} \right\rceil = \mathsf{S}s_{(m)} = \Delta^{N-(m+1)}\varepsilon_\gamma.$$

Choosing $m = N - 1$ yields $s_{(N-1)} = \Delta\varepsilon_\gamma$ and, consequently, $\mathsf{S}s_{(N-1)} = \mathsf{S}\left(\Delta\varepsilon_\gamma\right) = \varepsilon_\gamma - \varepsilon_\gamma\left[-K'\right] = \varepsilon_\gamma$. This in combination with modulo decomposition (2) yields $\gamma[k] = y[k] + \left(\mathsf{S}s_{(N-1)}\right)[k]$ and the proof is complete. □

4. NUMERICAL EXPERIMENTS

In our numerical experiments, we use the Walnut dataset from [16], which is transformed to parallel beam geometry with $M = 600$ and $K = 1128$ corresponding to $T = 1/1128$. Moreover, the Radon data is normalized to the dynamical range $[0, 1]$ so that $\|\mathcal{R}f\|_\infty = 1$. Its Modulo Projections are displayed in Fig. 2(a), where we use $\lambda = 0.001$ and $\Omega = 207$ so that $T \leq (2\Omega e)^{-1}$ is fulfilled.

The reconstruction with our proposed **US-FBP** method is shown in Fig. 2(b), where we use the cosine filter with

$$\mathcal{F}_1 F_\Omega(\omega) = |\omega| \cos\left(\frac{\pi\omega}{2\Omega}\right) \mathbb{1}_{[-\Omega,\Omega]}(\omega).$$

A related method to our problem is Phase Unwrapping (PU). However, redundancy plays a key role in our work which cannot be exploited with PU methods. Furthermore, PU cannot work with higher order differences. A detailed discussion on these aspects is presented in [10]. For comparison, we also applied PU in place of Unlimited Sampling for recovering p_θ from p_θ^λ. The result is displayed in Fig. 2(c). We observe that the PU-FBP method is not able to recover the walnut, whereas our method yields a reconstruction of the walnut that is competitive to the direct FBP reconstruction from conventional Radon data. In this example, the MRT is able to compress the dynamic range $\|\mathcal{R}f\|_\infty / (2\lambda)$ by about 500 times.

Remarks on Numerical Assessment. We first want to compare our US-FBP method of this work with the algorithm proposed in [8]. In this paper, we use that convolving a compactly supported g and a band-limited ϕ results in a λ-supported function so that $(g * \phi) \in \mathcal{B}_\lambda^\rho$ for a sufficiently large $\rho > 0$. With this, we are able to greatly reduce the necessary sample size for exact recovery from modulo samples. In our numerical tests we found that the walnut Radon Projections are λ-supported with $\rho = 1.6$. This yields $K' = 1815$ and for each angle we have to collect 2944 Modulo Radon Projections, which corresponds to an increase of sample size by 687 samples per angle. In contrast, the algorithm in [8] needs $\lceil 6/\lambda \rceil + N + 1 = 6011$ Modulo Radon Projections for each angle. This corresponds to an increase by 3754 samples per angle, which is more than 5-times the amount.

Secondly, we note that empirically the US-FBP method works with a much slower sampling rate T such that $T \leq (2\Omega e)^{-1}$ is *not* fulfilled. In the case of the walnut data, T is fixed but the bandwidth Ω can be varied. We found that the US-FBP method succeeds even for $\Omega = 600$, which is the maximal choice to ensure the condition $M \geq \Omega$ and leads to a sharper reconstruction of the walnut.

Finally, we remark that the proposed US-FBP method is *empirically stable* in the presence of noise. To demonstrate this, we added white Gaussian noise with SNR of 30 dB to the Modulo Radon Projections of the walnut with $\lambda = 0.075$, which leads to an RMSE of 1.2×10^{-3}. Algorithm 1 succeeds to recover the Radon Projections up to the same RMSE and the error between the US-FBP reconstruction and the FBP reconstruction from Radon data is 5×10^{-4}.

5. FUTURE WORK AND CONCLUSIONS

The problem of high dynamic range tomography is considered in this paper. This topic is still in the early stages of its investigation and recent examples of research efforts include [4–7]. In contrast, we proposed a solution that is based on the Modulo Radon Transform (MRT) [8]. The MRT encodes Radon Transform projections with modulo non-linearity and this ensures that the detector never saturates. A practical algorithm for inverting the MRT is proposed which works sequentially; first the effect of non-linearity is removed and then, filtered back projection is used of reconstruction. By introducing an approximate form of compact support, we substantially improve over the previously developed method for MRT in [8]. One of the key areas of improvement is that one can work with lesser sampling density. Our work raises a number of interesting questions related to tighter sampling guarantees, robustness with respect to noise and possibility of a MRT Fourier Slice Projection theorem that would avoid the need for a sequential recovery of images.

6. REFERENCES

[1] P. Funk, "Über eine geometrische Anwendung der abelschen Integralgleichung", *Mathematische Annalen*, vol. 77, no. 1, pp. 129–135, Mar. 1915.

[2] J. Radon, "Über die Bestimmung von Funktionen durch ihre Integralwerte längs gewisser Mannigfaltigkeiten", *Ber. Sächs. Akad. Wiss.*, vol. 69, pp. 262–277, Apr. 1917.

[3] A. M. Cormack, "Representation of a function by its line integrals, with some radiological applications", *Journal of Applied Physics*, vol. 34, no. 9, pp. 2722–2727, Sep. 1963.

[4] P. Chen, Y. Han, and J. Pan, "High-dynamic-range CT reconstruction based on varying tube-voltage imaging", *PLOS ONE*, vol. 10, no. 11, p. e0141789, Nov. 2015.

[5] Y. Li, Y. Han, and P. Chen, "X-ray energy self-adaption high dynamic range (HDR) imaging based on linear constraints with variable energy", *IEEE Photon. J.*, vol. 10, no. 1, p. 3400114, Feb. 2018.

[6] P. Eppenberger, M. Marcon, M. Ho, F. D. Grande, T. Frauenfelder, and G. Andreisek, "Application of a colored multiexposure high dynamic range technique to radiographic imaging", *Journal of Computer Assisted Tomography*, vol. 40, no. 4, pp. 658–662, Jul. 2016.

[7] J. T. Weiss, K. S. Shanks, H. T. Philipp, J. Becker, D. Chamberlain, P. Purohit, M. W. Tate, and S. M. Gruner, "High dynamic range x-ray detector pixel architectures utilizing charge removal", *IEEE Trans. Nucl. Sci.*, vol. 64, no. 4, pp. 1101–1107, Apr. 2017.

[8] A. Bhandari, M. Beckmann and F. Krahmer "The modulo Radon transform and its inversion", *in 28th European Signal Processing Conference (EUSIPCO)*, 2020.

[9] A. Bhandari, F. Krahmer, and R. Raskar, "On unlimited sampling", in *Intl. Conf. on Sampling Theory and Applications (SampTA)*, Jul. 2017, pp. 31–35.

[10] ——, "On unlimited sampling and reconstruction", arXiv:1905.03901, 2019.

[11] ——, "Methods and apparatus for modulo sampling and recovery," U.S. Patent US/20 190 103 876 A1, Apr., 2019.

[12] J. Rhee and Y. Joo, "Wide dynamic range CMOS image sensor with pixel level ADC", *Electron. Lett.*, vol. 39, no. 4, p. 360, 2003.

[13] A. Bhandari, F. Krahmer, and R. Raskar, "Unlimited sampling of sparse signals," in *IEEE Intl. Conf. on Acoustics, Speech and Sig. Proc. (ICASSP)*, Apr. 2018.

[14] ——, "Unlimited sampling of sparse sinusoidal mixtures," in *IEEE Intl. Sym. on Information Theory (ISIT)*, Jun. 2018.

[15] F. Natterer and F. Wübbeling, "Mathematical Methods in Image Reconstruction", SIAM, Philadelphia, 2001.

[16] K. Hämäläinen, L. Harhanen, A. Kallonen, A. Kujanpää, E. Niemi, and S. Siltanen, "Tomographic X-ray data of a walnut", Zenodo, 2015. http://doi.org/10.5281/zenodo.1254206